European Journal of Immunology

Immunity to infection

Basic

Research Article

Rotavirus infection causes mesenteric lymph node hypertrophy independently of type I interferon or TNF-α in mice

Joy Nakawesi[1], Getachew Muleta Konjit[1], Dragos-Christian Dasoveanu[2], Bengt Johansson-Lindbom[1,3] and Katharina Lahl[1,3]

[1] Immunology Section, Lund University, Lund, Sweden
[2] Department of Immunology, University of Toronto, Toronto, Ontario, Canada
[3] Division of Biopharma, Institute for Health Technology, Technical University of Denmark (DTU), Kongens, Denmark

Lymphoid organ hypertrophy is a characteristic feature of acute infection and is considered to enable efficient induction of adaptive immune responses. Accordingly, oral infection with rotavirus induced a robust increase in cellularity in the mesenteric LNs, whose kinetics correlated with viral load and was caused by halted lymphocyte egress and increased recruitment of cells without altered cellular proliferation. Lymphocyte sequestration and mesenteric LN hypertrophy were independent of type 1 IFN receptor signaling or the continuous presence of TNF-α. Our results support previous findings that adaptive immunity toward rotavirus is initiated primarily in the mesenteric LNs and show that type I IFN or TNF-α are not required to coordinate the events involved in the LN response.

Keywords: rotavirus · lymphoid organ hypertrophy · type I interferon · TNF-α

Additional supporting information may be found online in the Supporting Information section at the end of the article.

Introduction

Naïve lymphocytes recirculate continuously between the blood and secondary lymphoid organs, which they enter via high endothelial venules, before spending several hours migrating randomly in the search for antigen. In the absence of cognate antigen, lymphocytes exit into the lymph and eventually return to the bloodstream through the thoracic duct [1–4]. Under steady-state conditions, lymph node (LN) cellularity is strictly controlled [5], but this changes during infection or inflammation, when alterations in leukocyte trafficking lead to transient hypertrophy of the local LNs [6–10]. In part, this reflects increased recruitment of lymphocytes due to remodeling and expansion of the high endothelial venules network mediated by VEGF produced by migratory dendritic cells (DCs) responding to PAMPS. In parallel, lymphocytes recognizing antigen transported from inflamed tissue by DCs become trapped in the draining LN and begin to proliferate. Finally, the exit of lymphocytes from the LN into the efferent lymph is blocked transiently, a process referred to as LN shutdown. By facilitating serial and long-lasting encounters between specific lymphocytes, DCs, and cognate antigen, LN hypertrophy is crucial for the efficient priming of adaptive immune responses [10–14].

A number of important players have been implicated in the coordination of LN hypertrophy, including type I IFN [15,16], TNF-α [17,18], IL-6 [19], complement [9], sphingosine-1 phosphate (S1P) [20], and β2 adrenergic receptor signaling [21]. However, the mechanisms involved in the response to specific pathogens in an anatomically defined tissue such as the intestine

Correspondence: Dr. Katharina Lahl
e-mail: klah@dtu.dk

are still poorly defined. Indeed, it has been reported that the hypertrophy and shutdown of lymphocyte egress in Peyer's patches (PPs) after infection with *Salmonella* was independent of type I IFN, TNF-α, and S1P [22]. As type I interferons (IFN-α/β) and TNF-α play pivotal roles in the priming of adaptive immune responses to viral infections including rotavirus (RV) [23–26], here we have examined the roles of these mediators in the context of murine RV infection of the intestine. We and others have shown previously that this model leads to temporary accumulation of B cells in the mesenteric LNs (mLNs) [27–29] and that the infection is controlled by coordinated activation of T-cell-dependent antibody production and $CD8^+$ T-cell mediated immunity [27,28,30,31]. Our results show that RV infection induces hypertrophy of the local secondary lymphoid organs (mLN, PP), with accumulation of all major circulating lymphocyte populations. mLN hypertrophy was associated with decreased lymphocyte egress and increased recruitment of cells, but without substantial local proliferation. The LN hypertrophy was independent of specific antigen receptor-, type 1 IFN receptor (IFNAR)-, or TNF receptor (TNFR)-mediated signaling, indicating that further work is needed to elucidate the mechanisms of LN shutdown in response to intestinal pathogens.

Results

RV-induced hypertrophy occurs primarily in the mLNs

We have previously reported that RV infection triggers a transient, threefold increase in total B-cell numbers in the mLNs between days 4 and 7, returning to baseline levels by day 8 postinfection [27]. To define the extent of this phenomenon in more detail, we monitored the changes in all hematopoietic cells in different lymphoid tissues over time in the model of oral RV infection in adult C57Bl/6 mice. As expected, the mLNs of RV-infected mice increased in size compared with uninfected mice between days 4 and 7 postinfection, with an approximately threefold increase in the total cellularity and in live $CD45^+$ cells (Fig. 1A and B). This hypertrophy was focused mainly to the mLNs, as there was only a small increase in $CD45^+$ cells in PPs on day 5 and there were no changes in the cellularity of spleen or brachial LNs used as a representative peripheral LN (pLN). The cellularity of the BM also remained constant over the course of infection (data not shown).

The mechanisms driving LN hypertrophy in response to viral infection have not been studied in detail before. Flow cytometric analysis of the lymphocyte populations at day 5 postinfection showed significantly increased numbers of both B and T lymphocytes in the mLNs of RV-infected mice (Fig. 1B). The accumulation of B cells was slightly more pronounced than that of T cells, possibly reflecting the generally longer dwell-time for B cells in lymphoid organs [32]. The RV-driven accumulation of B, $CD4^+$, and $CD8^+$ T lymphocytes in the mLNs involved both naive and activated/effector cells (Fig. 1C).

Together, these findings suggest that the bulk of the adaptive immune response against RV in adult mice is initiated in the mLN and gut-associated lymphoid tissues and is not associated with global changes in lymphocyte population dynamics in other tissues. The hypertrophy of mLNs is associated with accumulation of $CD4^+$ and $CD8^+$ T cells of both naïve and activated/effector phenotypes.

Lymphocyte accumulation during RV infection in the mLNs does not require antigen-specific activation

Lymphocyte retention in secondary lymphoid organs involves a failure to respond to the gradient between the levels of sphingosine-1-phosphate in the bloodstream and tissue [33]. As one of the main ways this can occur is due to antigen-receptor engagement that leads to downregulation of the sphingosine-1-phosphate receptors 1 and 3 (S1PR1 and S1PR3) on responding lymphocytes [33], we examined whether the lymphocyte accumulation in mLNs required recognition of cognate antigen. To do this, we used a B-cell receptor-specific mouse model, Switching anti-HEL (SW_{HEL}), which contain B cells that are specific for hen egg lysozyme (HEL) and so will not receive a BCR signal upon RV infection, unlike some of the remaining polyclonal B cells [34]. Five days after RV infection, total and naïve (IgD^+) HEL^+ and HEL^- B cells accumulated equally in the mLNs (Fig. 2A and B). In contrast, only HEL^- B cells contributed to the increase in antigen-experienced (IgD^-) B cells and $CD138^+$ plasmablasts seen after RV infection, while the HEL-specific B cells did not (Fig. 2C and D). Thus, antigen-specific recognition is dispensible for the accumulation of B lymphocytes in the mLNs after RV infection, but is needed for these cells to class switch and differentiate into plasmablasts. A similar independence of antigen recognition by T cells for PP hypertrophy was shown previously in the context of Salmonella infection [22].

Cellular mechanisms of RV-induced LN hypertrophy

We next investigated whether the mLN hypertrophy during RV infection reflected increased cell proliferation, increased cell entry from the blood, or increased mLN retention. To address the role of proliferation, we transferred Cell Trace Violet (CTV)-labeled splenocytes into C57Bl/6 mice 1 day before oral infection with RV and examined CTV dilution as a measure of cell division among transferred cells. Transferred $CD4^+$ and $CD8^+$ T and B cells could be found in the mLNs, with their accumulation being increased equally by the presence of infection and their proportions remaining similar in uninfected and infected LNs (Fig. 3A and B). Very few (<10%) of the transferred T or B cells found in mLNs had undergone cell division and there were only small and transient increases in cell division in response to infection (Fig. 3C).

To investigate lymphocyte recruitment into the mLNs in response to RV, we transferred $CD45.1^+$ splenocytes into $CD45.2^+$ C57Bl/6 mice on day 5 postinfection and assessed their numbers 4 h later to avoid confounding effects of cell egress [35]. As spleen cell numbers remained constant after RV infection, we normalized

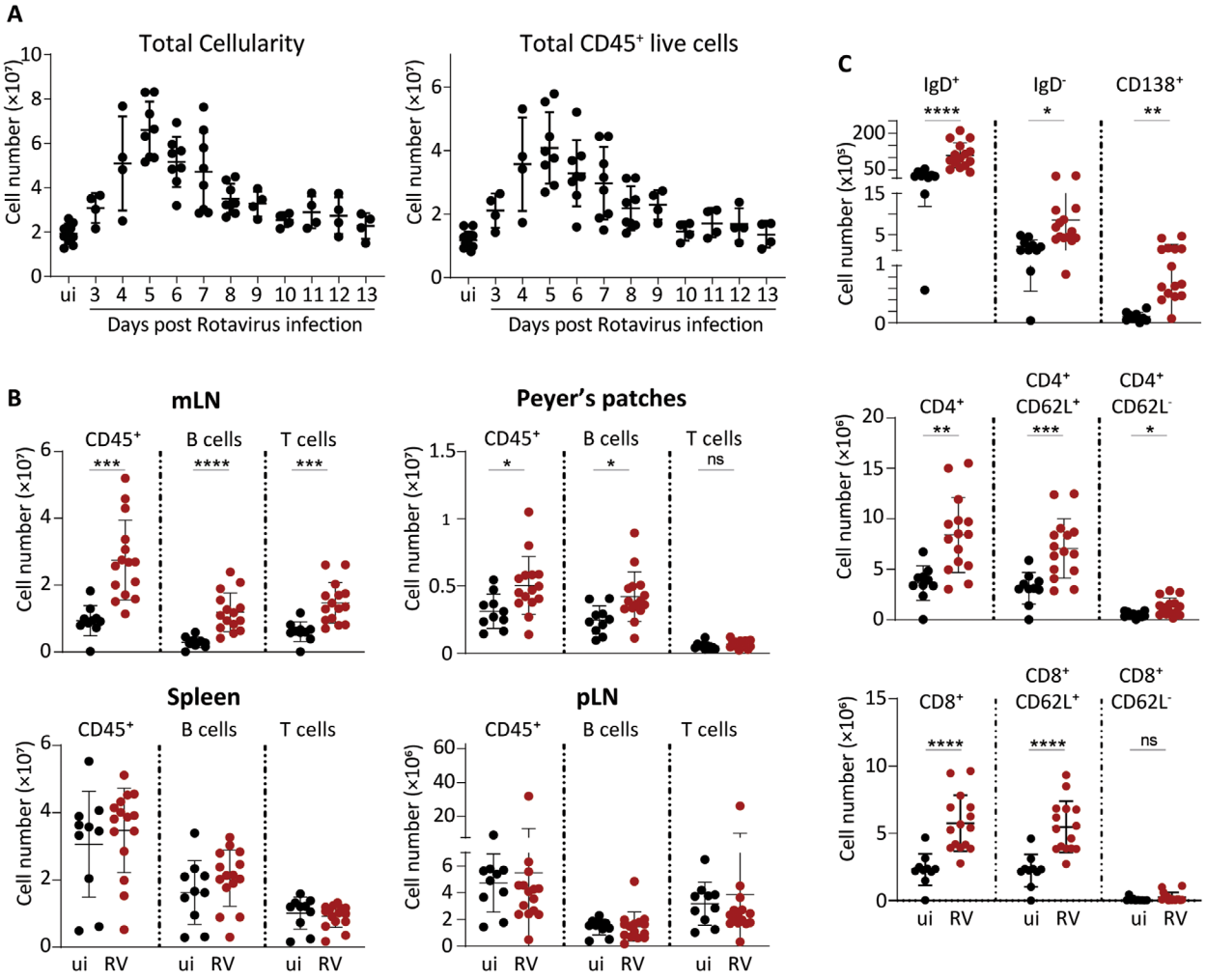

Figure 1. RV-induced lymphoid organ hypertrophy occurs primarily in the mLNs. C57Bl/6 mice were infected orally with RV. (A) Total mLN cellularity (left) and total number of CD45$^+$ live cells (right) was monitored daily from 3-13 days after RV infection. (B) Total number of CD45$^+$ live cells, B cells (live CD45$^+$CD19$^+$B220$^+$), and T cells (live CD45$^+$TCRβ$^+$) in the mLNs, PP, spleen, and pLNs (brachial LNs) on day 5 after RV infection. (C) Total number of lymphocyte subsets in mLNs on day 5 after RV infection-naïve B cells: live CD45$^+$CD19$^+$B220$^+$IgD$^+$, antigen-experienced B cells: live CD19$^+$B220$^+$IgD$^-$, CD138$^+$ plasmablasts: live CD19$^+$IgD$^-$CD138$^+$ (top panel), total CD4$^+$ T cells: live CD45$^+$TCRβ$^+$CD4$^+$, naïve CD4$^+$ T cells: live CD45$^+$TCRβ$^+$CD4$^+$CD62L$^+$, antigen-experienced CD4$^+$ T cells: live CD45$^+$TCRβ$^+$CD4$^+$CD62L$^-$ (middle panel) and total CD8$^+$ T cells: live CD45$^+$TCRβ$^+$CD8$^+$, naïve CD8$^+$ T cells: live CD45$^+$TCRβ$^+$CD8$^+$CD62L$^+$, antigen-experienced CD8$^+$ T cells: live CD45$^+$TCRβ$^+$CD8$^+$CD62L$^-$ (lower panel). See Supporting Information Fig. S1 for gating strategy. All data were measured by flow cytometry. Data are pooled from (A) one or two ($n = 4$ mice each experiment, repeat only for days 5–8), (B and C) three ($n = 3$–4 mice each experiment) independent experiments. Error bars show mean ± 1 SEM. One-way ANOVA, Tukey's post hoc. $^*p < 0.05$, $^{**}p < 0.01$, $^{***}p < 0.001$. Symbols (B and C): black: uninfected control (ui); red: RV infected. Dots represent individual mice.

the numbers of cells recovered from other tissues to those found in the spleen. The results showed that more transferred lymphocytes were found in both the mLNs and PPs of infected mice compared with those in uninfected controls, whereas there was no change in recruitment to peripheral LNs (Fig. 3D).

We next addressed whether retention of lymphocytes within the mLN was altered following RV infection by blocking entry into the mLN using αCD62L blocking antibody at day 4 after infection. As expected, the overall mLN cellularity was significantly decreased in uninfected control mice 24 hours after blocking cell influx (Fig. 4A). In the context of RV infection, this decrease was somewhat less pronounced despite the underlying hypertrophy (Fig. 1) and the known positive correlation between overall LN cellularity and exit rates [36]. In accordance with a previously reported longer dwell-time of B cells compared to T cells [32], B cells were more efficiently retained in both infected and uninfected mice, leading to an overall higher ratio of B cells over T cells upon blockade of lymphocyte entry (Fig. 4B–D). The retained IgD$^-$ B-cell compartment containing class-switched cells was significantly enriched in mLNs from RV-infected mice and not affected by entry blockade (Fig. 4B) and this was also the case for CD138$^+$ plasmablasts (data not shown). The effect on retention of CD4$^+$ T cells by RV infection was minor, but CD8$^+$ T cells were significantly better retained in the context of infection (Fig. 4C).

Thus, infection with RV leads to increased recruitment of lymphocytes into and enhanced retention within intestinal lymphoid

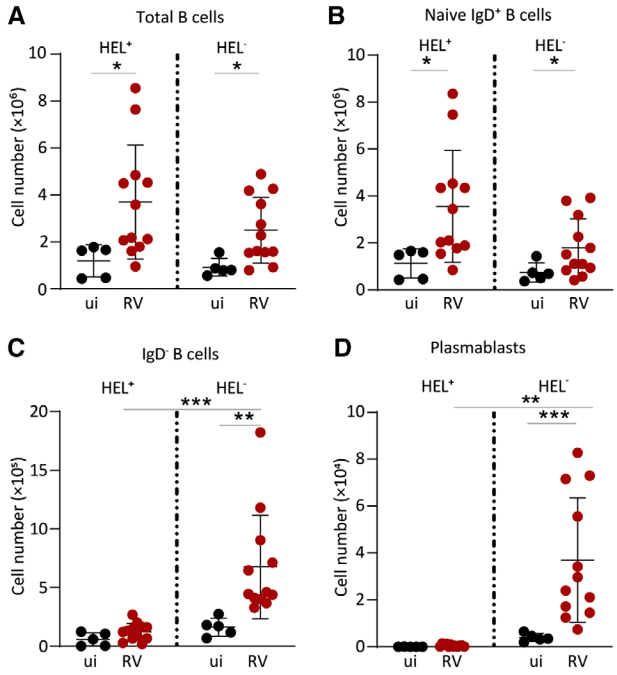

Figure 2. B lymphocyte accumulation during RV infection does not require cell intrinsic antigen-specific activation. Switching anti-HEL (SW_{HEL}) mice were infected orally with RV and mLNs were analyzed on day 5 after infection. (A) Total number of HEL^+ and HEL^- B cells (live $CD45^+CD19^+B220^+HEL^{+/-}$). (B) Naïve B cells (live $CD45^+CD19^+B220^+HEL^{+/-}IgD^+$). (C) Antigen-experienced B cells (live $CD19^+B220^+HEL^{+/-}IgD^-$). D) $CD138^+$ plasmablasts (live $CD45^+CD19^+B220^+HEL^{+/-}IgD^-CD138^+$). For full gating strategy, see Supporting Information Fig. 2. All data were measured by flow cytometry. Data are pooled from three (n = 2–4 mice each experiment) independent experiments. Error bars show mean ± 1 SEM. One-way ANOVA, Tukey's post hoc. $^*p < 0.05$, $^{**}p < 0.01$, $^{***}p < 0.001$. Symbols: black: uninfected control (ui); red: RV infected. Dots represent individual mice.

tissues, whereas local proliferation plays very little role in the lymphoid hypertrophy.

RV-induced mLN hypertrophy is independent of IFNAR signaling or TNF-α

The early type 1 IFN-induced activation marker CD69 limits cell egress during the early phase of an immune response by causing internalization of S1PR1, and thus abrogating the chemotactic stimulus for lymphocyte exit [10,11,37]. To assess the impact of type I IFN signaling on mLN hypertrophy during RV infection, we assessed the lymphocyte populations in the mLNs 5 days postinfection in $IFNAR^{KO}$ mice. At steady state, $IFNAR^{KO}$ mice showed a trend toward fewer total live $CD45^+$, B and T cell numbers compared with age- and sex-matched WT controls (Fig. 5A). However, the RV-induced increases in the numbers of all lymphocyte populations, including IgD^{neg} B cells and plasmablasts in mLN, were not affected by absence of type 1 IFNR signaling (Fig. 5A–C). As we have reported previously [23], the upregulation of CD69 on lymphocytes in response to RV infection was dependent on IFNAR signaling (Fig. 5D).

TNF-α has also been shown to mediate LN hypertrophy in response to immunologic triggers [12,17–19,38,39]. To investigate whether TNF-α played a role in RV-induced shutdown of the mLNs, C57Bl/6 mice were infected orally with RV and TNF-α was blocked by administration of antibody on days 3 and 4 after infection. This did not affect the expansion of lymphocyte subsets in the mLNs (Fig. 6A). To test whether TNF-α signaling was instead required for early recruitment into the mLN, we infected mice double-deficient for the TNFR1/2 receptors. Again, mLN cellularity increased upon RV infection regardless of whether TNFR signaling was intact or not (Fig. 6B), paralleling previous findings in PPs of *Salmonella*-infected mice [22].

Together these results show that the enhanced lymphocyte sequestration in the mLNs in response to RV is independent of the type 1 IFN–CD69–S1PR1 axis and of TNF-α.

Discussion

Lymphoid organ hypertrophy is a central component of immune activation and is considered to be essential for efficient induction of adaptive immune responses [20,40]. As its kinetics and extent correlate directly with the level of innate stimulation (this study and [27]), a better understanding of the mechanisms would be crucial for improving vaccine design and ensuring effective immune memory. By analyzing the kinetics and location of lymphoid hypertrophy in response to oral RV infection in adult mice, we found that this reaction was confined mostly to the LNs draining the intestines, with no response in more distal lymphoid tissues including the spleen. This is consistent with previous findings that adaptive immunity to RV is coordinated primarily in the mLNs [27,28,41]. Interestingly, there was also comparatively little reaction in PP, perhaps additionally reflecting the fact that this tissue is under constant stimulation from luminal contents and hence less able to respond strongly above an already high baseline.

Schulz et al. reported that retention is the major contributor to PP hypertrophy in response to *Salmonella* infection [22]. In agreement, lymphocyte proliferation did not substantially add to the overall cellularity of the mLN during RV infection. In addition to enhanced retention, we however detect a somewhat increased recruitment of lymphocytes to the draining LNs, suggesting that hypertrophy during RV infection does not exclusively result from augmented retention of lymphocytes in our enteric viral infection model. Hence, since recruitment and retention are uncoupled events in the context of inflammation-induced hypertrophy [7,42], RV infection influences the process on at least two different levels.

There is considerable evidence that the IFNAR-CD69-S1PR1 pathway is the major mechanism underlying lymphoid organ hypertrophy [10,11,37] and it has been shown that antigenic stimulation of specific lymphocytes leads to rapid downregulation of S1PR, disabling their responses to the S1P gradient from the bloodstream and retaining them in the lymphoid organ [20,33]. However, in our studies using RV-infected SW_{HEL} mice, the

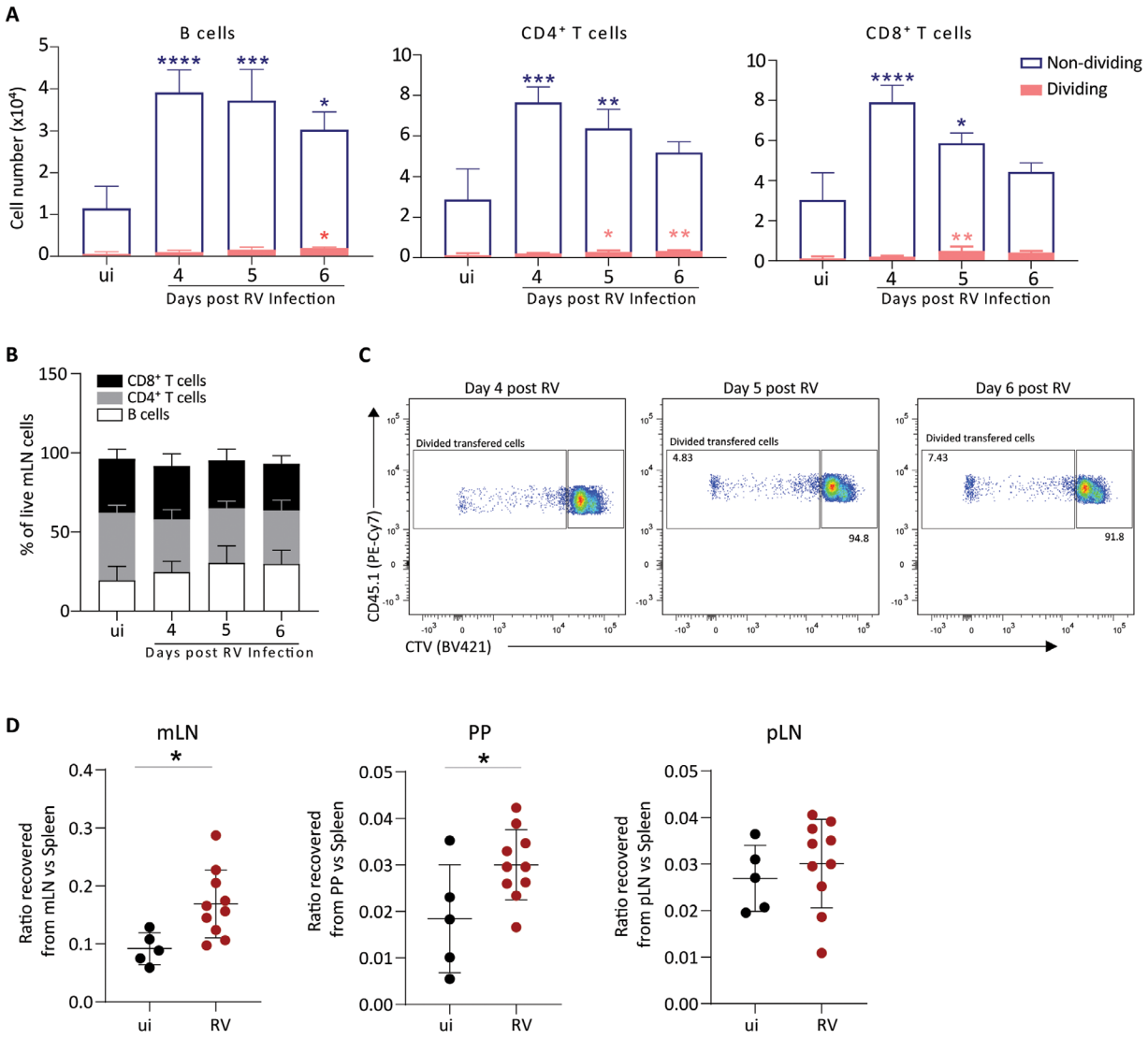

Figure 3. Lymphocyte proliferation is not a major contributor to RV-induced LN hypertrophy. Cell Trace Violet labeled total splenocytes were adoptively transferred into C57Bl/6 WT mice that were infected orally with RV 1 day later. (A) Numbers of dividing and nondividing transferred lymphocytes recovered from mLNs on the indicated days postinfection: B cells (live CD45.1$^+$CD19$^+$B220$^+$), CD4$^+$ T cells (live CD45.1$^+$TCRβ$^+$CD4$^+$), and CD8$^+$ T cells (live CD45.1$^+$TCRβ$^+$CD8$^+$). (B) Relative composition of dividing and nondividing lymphocytes in mLN during RV infection. (C) Representative flow cytometry plots showing CTV staining of transferred total CD45.1$^+$ cells in the mLNs during RV infection. B cells stain brighter for CTV than T cells, resulting in a double peak for undivided cells. The gating strategy including separate CTV staining plots for B cells and CD4$^+$ and CD8$^+$ T cells are provided in Supporting Information Fig. S3. (D) Lymphocyte entry into lymphoid organs during RV infection. 10^7 WT spleen cells were transferred into infected and uninfected congenic recipients and lymphoid organs were analyzed 4 h later. The numbers of cells recovered were normalized to those from the spleen. All data were measured by flow cytometry. Data are pooled from (A) and (D) two (n = 2–7 mice each experiment) independent experiments. (B) and (C) data from one representative experiment out of two independent experiments (n = 3–4 mice each experiment). Error bars show mean ± 1 SEM. (D) Unpaired t test. $^*p < 0.05$, $^{**}p < 0.01$, $^{***}p < 0.001$. Symbols: uninfected control; black symbols and RV infected; red symbols.

retention of lymphocytes in mLN did not require recognition of cognate antigen, showing that LN hypertrophy is global and not dominated by the retention of antigen-specific lymphocytes. Furthermore, we found that the mLN hypertrophy in this model did not require type I IFN signaling, despite the expected reduction of CD69 expression by B and T cells in infected IFNAR-deficient mice compared with controls. This supports the previous notion of a lack of a retention phenotype in CD69-deficient mice [43] and matched findings using a *Salmonella* infection model causing PP hypertrophy by Schulz et al. [22]. Together, these data suggest that mechanisms that regulate overall LN cellularity during a viral infection might differ from those coordinating retention of responding antigen-specific lymphocytes, as suggested previously [22].

Our studies using antibody-mediated blocking of TNF-α at the time of RV infection and TNFR1/2-deficient mice showed that TNF-α signaling was also dispensable for mLN hypertrophy in response to RV infection. This contrasts with previous findings

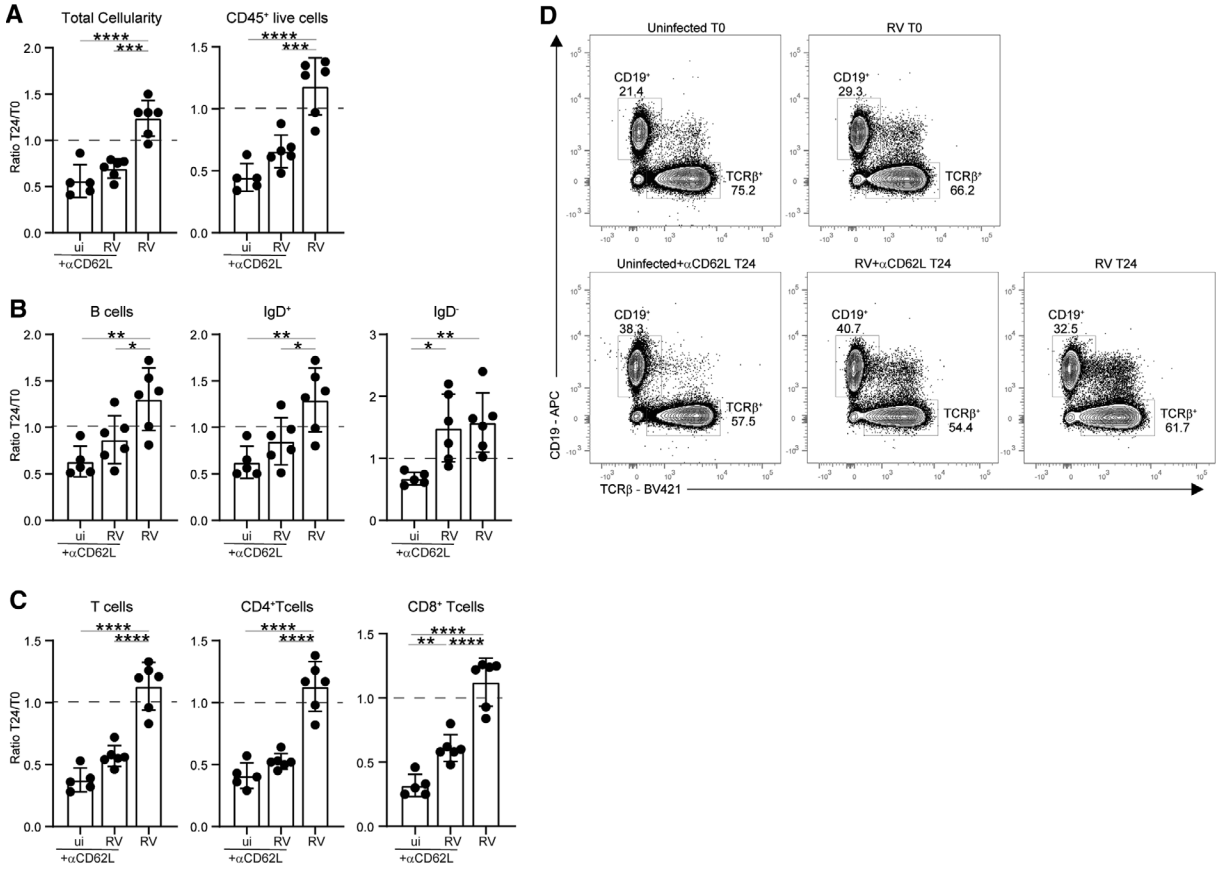

Figure 4. Lymphocyte retention contributes to RV-induced LN hypertrophy. C57Bl/6 WT mice were infected orally with RV. On day 4 after RV infection, some of the uninfected (ui) and RV-infected mice were sacrificed (T0). The remaining group received anti-CD62L blocking antibody to block further lymphocyte entry into the LNs or PBS and was taken down after 24 h later (T24 = day 5 after RV infection). Lymphocyte retention within the mLNs was assessed as the ratio of cells present in the mLNs at T24 over the mean lymphocyte population present at baseline (T0, individually assessed for uninfected and infected groups). (A) Total mLN cellularity (left) and total number of $CD45^+$ live cells (right). (B) Total B cells (live $CD45^+CD19^+B220^+$), naïve B cells (live $CD45^+CD19^+B220^+IgD^+$) and antigen-experienced B cells (live $CD19^+B220^+IgD^-$). (C) Total T cells (live $CD45^+TCR\beta^+$), $CD4^+$ T cells (live $CD45^+TCR\beta^+CD4^+$), and $CD8^+$ T cells (live $CD45^+TCR\beta^+CD8^+$). D) Representative flow cytometry plots showing B cell ($CD19^+$) versus T cell ($TCR\beta^+$) frequencies in both control and RV infected mice upon anti-CD62L blocking in the mLNs. All data were measured by flow cytometry. Data are pooled from two independent experiments with two to three mice per experiment. Error bars show mean ± 1 SEM. One-way ANOVA, Tukey's post hoc. $^*p < 0.05$, $^{**}p < 0.01$, $^{***}p < 0.001$.

indicating that TNF-α can increase the influx of lymphocytes into draining LN and, in some cases, can also block lymphocyte exit [17–19,39,44]. In addition, TNF-α signaling can drive migration of peripheral DC to the draining LN at steady state or in response to the TLR ligands poly(I:C) or R848 [45–48]. However, LN hypertrophy induced by *Anopheles* mosquito bite is independent of TNF-α [49] and genetic ablation of the TNFR1 has no effect on the PP hypertrophy observed in response to *Salmonella* infection [22]. Furthermore, TNF-α was found to be dispensable for DC migration and LN swelling induced by subcutaneous injection of bacterial peptidoglycan [50]. Thus, the exact role of TNF-α in LN hypertrophy may be stimulus and location dependent and remains to be defined more precisely.

It would be important to assess the role of type I IFN and TNF-α in the accumulation of antigen-specific T and B cells in response to RV, as previous work has shown that while the retention of polyclonal lymphocytes in PP in response to *Salmonella* infection is TNF-α/type I IFN independent, a type I IFN-CD69-S1PR1-dependent mechanism is required to retain activated antigen-specific T cells [22,51]. Other mechanisms that may play a role in the RV-induced LN response include signaling via β2-adrenergic receptors (β2ARs) expressed on lymphocytes, which can inhibit egress of lymphocytes from LNs and lead to hypertrophy of the draining LNs in response to mouse CMV infection [52]. In support of this idea, enteric infection with *Salmonella* has been shown to activate β2ARs in muscularis macrophages [53] and thus it would be interesting to investigate the role of β2ARs in the LN response to RV.

It has long been appreciated that lymphocyte exit into the efferent lymph is not a random event [54]. Identifying the drivers of the global, unspecific lymphoid organ shutdown will pave the way for better understanding its physiological consequences, possibly including enhanced encounter of antigen by naïve T cells, promotion of memory formation of responding lymphocytes and barrier functions to contain infectious agents on site.

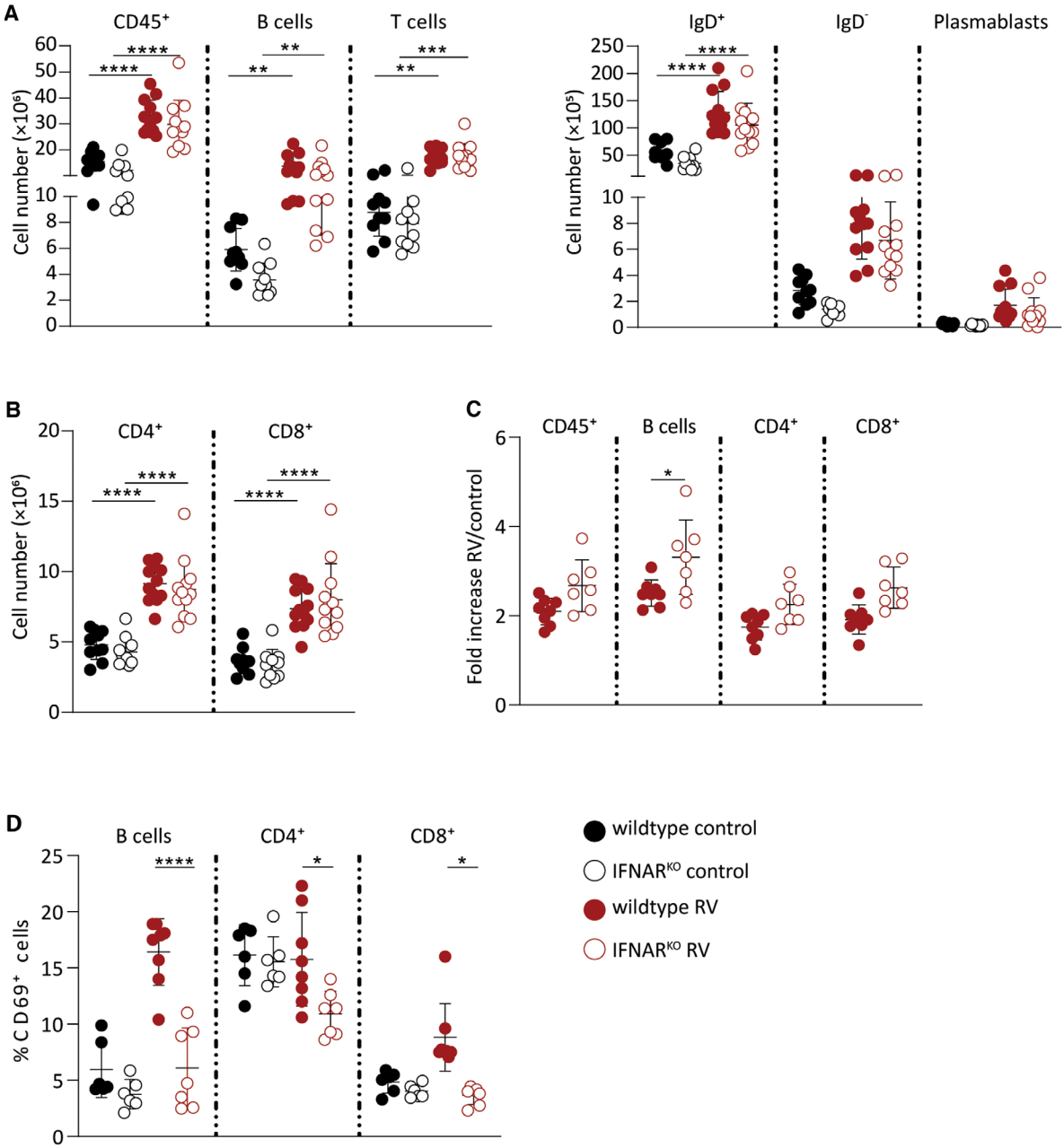

Figure 5. Lymphocyte sequestration in mLNs from RV-infected mice is independent of the type 1 IFN receptor. IFNAR^{KO} and WT mice were infected orally with RV and the lymphocyte populations in the mLNs were analyzed 5 days later. (A and B) Total number of CD45$^+$ live cells, B cells (live CD45$^+$CD19$^+$B220$^+$), and T cells (live CD45$^+$TCRβ$^+$); lymphocytes were further subgated into IgD$^+$, IgD$^-$, CD138$^+$ (for B cells), and CD4$^+$ and CD8$^+$ (for T cells). (C) Fold change of cell numbers in RV-infected tissues compared with uninfected controls. (D) Percentage of CD69$^+$ cells within the designated subsets. All data were measured by flow cytometry. Data are pooled from two independent experiments ($n = 3$–5 mice each experiment). (D) One representative experiment out of two independent experiments (n = 3–5 mice each experiment). Error bars show mean ± 1 SEM. (A, B, and D) One-way ANOVA, Tukey's post hoc. $^*p < 0.05$, $^{**}p < 0.01$, $^{***}p < 0.001$, $^{****}p < 0.0001$. (C) Unpaired *t* test. $^*p < 0.05$.

Material and methods

Mice

All mice were on the C57Bl/6 background. Littermate or age-matched mice were used for all experiments. Male and female mice were used between 8 and 12 weeks of age. Wild-type C57Bl/6NRj mice were purchased from Janvier Labs, Saint Berthevin Cedex, France and were acclimatized for at least 1 week in the animal facility at Lund University before use. CD45.1 congenic mice (B6.SJL-Ptprca Pepc^b/BoyJ, Jackson Laboratories), B6(Cg)-*Ifnar1*$^{tm1.2Es/J}$ (IFNAR^{KO}; 028288, Jackson Laboratories), Tnfrsf1-dKO mice (TNFR1/2$^{-/-}$) [55], and Switching anti-HEL

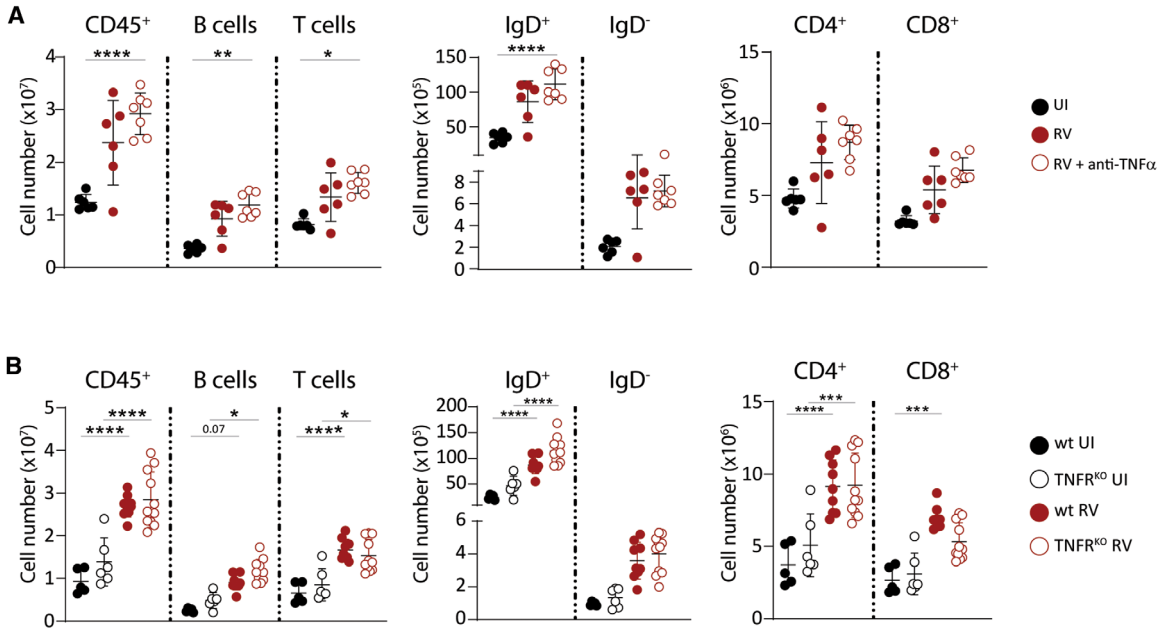

Figure 6. Lymphocyte sequestration in RV-infected mLNs is independent of TNF-α. C57Bl/6 WT mice were infected orally with RV and TNF-α was blocked on day 3 and 4 post RV infection by injection of anti-TNF-α antibody (A) or TNFR1/2^{KO} were infected orally with RV (B). The lymphocyte populations in the mLNs were analyzed on day 5 postinfection. (A and B) Total number of CD45$^+$ live cells, B cells (live CD45$^+$CD19$^+$B220$^+$), and T cells (live CD45$^+$TCRβ$^+$), lymphocytes were further subgated on IgD$^+$, IgD$^-$, CD138$^+$ (for B cells), and CD4$^+$ and CD8$^+$ (for T cells). All data were measured by flow cytometry. Data pooled from two (A: n = 3–4, B = 2–6 mice each experiment) independent experiments. Error bars show mean ± 1 SEM. One-way ANOVA, Tukey's post hoc. $^*p < 0.05$, $^{**}p < 0.01$, $^{***}p < 0.001$.

mice (SW_{HEL}) [34] were bred and maintained in the Clinical Research Center at Lund University. All animal experiments were performed under the animal care and use regulations of the Lund/Malmö Animal Ethics Committee.

Rotavirus Infections

The virulent WT EC_w strain of RV was obtained from cleared intestinal homogenates of suckling mice that had been infected orally with RV at 3 days of age and sacrificed 2 days after infection. For infection of adult mice, RV was inoculated orally at a dose of 3×10^3 diarrhea-inducing dose 50 (DD_{50}) and lymphoid organs were collected at the indicated days after infection for isolation of lymphocytes.

Cell isolation and flow cytometry

Single-cell suspensions from mLNs, Peyer's patches, brachial LNs, and spleen were generated by mechanical disruption through a 70 μm cell strainer into MACS buffer (5% FBS, 500 mL PBS and 0.05M EDTA [Gibco]). Nonspecific binding was blocked with normal rat serum (Sigma) and rat anti-mouse CD16/CD32 Fc block (2.4G2, BD Biosciences) for 20 min at 4°C. The following antibodies were used: anti-CD19 (1D3), anti-CD138 (281-2), anti-B220 (RA3-6B2), anti-IgD (11-26c.2a), anti-CD45 (30-F11), anti-CD45.1 (A20), anti-CD45.2 (104) (BioLegend), anti-CD62L (MEL-14) (eBioscience), anti-CD69 (H1.2F3), anti-CD4 (RM4-4), anti-CD8α (53-6.7), anti-TCRβ (H57-597), and PI (P4864-10ML, Sigma-Aldrich) was used to assess cellular viability. The CellTrace™ Violet Cell Proliferation Kit was used according to the manufacturer's protocol for in vitro labeling of total splenocytes (C34557, Invitrogen by Thermo Fisher Scientific).

Data acquisition was performed using an LSRII cytometer and DIVA software (BD Bioscience). The analysis was performed using FlowJo software 10 (Treestar Inc).

TNF-α and CD62L blocking

To block TNF-α in vivo, mice were injected with 0.3 mg of anti-TNF-α (XT3.11; BioXcell) antibody intravenously on days 3 and 4 after RV infection. We used 100 μg/mouse InVivoMAb anti-mouse L-Selectin antibody (CD62L, clone Mel-14, BioXcell) i.p. on day 4 post-RV infection to block further entry of circulating lymphocytes into LNs without affecting lymphocyte egress from LNs. Control mice received PBS (Gibco).

Statistical analysis

Unless otherwise stated, data are shown as mean ± 1 SD and statistical significance was calculated by one-way ANOVA with Tukey's multiple comparison using GraphPad Prism software (GraphPad).

Acknowledgements: We thank the Lahl and Agace laboratories for many fruitful discussions and Dr. Allan Mowat for editing of the manuscript. KL was supported by a Vetenskapsrådet Young Investigator Award (2014-3595), the Ragnar Söderberg Foundation Fellowship in Medicine, a Lundbeck Foundation Research Fellowship, the Åke Wiberg Foundation, the Carl Trygger Foundation, and the Crafoord Foundation. KL and JN received project funding from the Royal Physiographic Society of Lund. The flow cytometer at Lund University was purchased with funding from the Lundberg Foundation. We thank Dr. Pronk for sharing TNFR1/2$^{-/-}$ mice. KL was supported by a Vetenskapsrådet Young Investigator Award (2014-3595), the Ragnar Söderberg Foundation Fellowship in Medicine, a Lundbeck Foundation Research Fellowship, the Åke Wiberg Foundation, the Carl Trygger Foundation, the Apotekare Hedbergs Foundation, and the Crafoord Foundation.

Conflict of interest: The authors declare no commercial or financial conflict of interests.

Peer review: The peer review history for this article is available at https://publons.com/publon/10.1002/eji.202048990.

Data availibility statement: The data that support the findings of this study are available from the corresponding author upon reasonable request.

References

1 **Girard, J. P. and Springer, T A.**, High endothelial venules (HEVs): specialized endothelium for lymphocyte migration. *Immunol. Today* 1995. **16**: 449–457.

2 **Mackay, B.**, **Marston, W. L. and Dudler, L.**, Naive and memory T cells show distinct. *J. Exp. Med.* 1990. **171**: 801–817.

3 **Grigorova, I. L.**, **Panteleev, M. and Cyster, J G.**, Lymph node cortical sinus organization and relationship to lymphocyte egress dynamics and antigen exposure. *Proc. Natl. Acad. Sci. USA* 2010. **107**: 20447–20452.

4 **Mandl, J. N.**, **Liou, R.**, **Klauschen, F.**, **Vrisekoop, N.**, **Monteiro, J. P.**, **Yates, A. J.**, **Huang, A. Y. et al.**, Quantification of lymph node transit times reveals differences in antigen surveillance strategies of naïve CD4+ and CD8+ T cells. *Proc. Natl. Acad. Sci. USA* 2012. **109**: 18036–18041.

5 **Mionnet, C.**, **Sanos, S. L.**, **Mondor, I.**, **Jorquera, A.**, **Laugier, J. P.**, **Germain, R. N. and Bajénoff, M.**, High endothelial venules as traffic control points maintaining lymphocyte population homeostasis in lymph nodes. *Blood*. 2011. **118**: 6115–6122.

6 **Hall, J. G. and Morris, B.**, The immediate effect of antigens on the cell output of a lymph node. *Br. J. Exp. Pathol.* 1965. **46**: 450–454.

7 **Cahill, R. N. P.**, **Frost, H. and Trnka, Z.**, The effects of antigen on the migration of recirculating lymphocytes through single lymph nodes. *J. Exp. Med.* 1976. **143**: 870–888.

8 **Stingl, G.**, **Katz, S. I.**, **Clement, L.**, **Green, I. and Shevach, E. M.**, Immunologic functions of Ia-bearing epidermal Langerhans cells. *J. Immunol.* 1978. **121**: 2005–2013.

9 **McConnell, I. and Hopkins, J.**, Lymphocyte traffic through antigen-stimulated lymph nodes. I. Complement activation within lymph nodes initiates cell shutdown. *Immunology* 1981. **42**: 217–223.

10 **Shiow, L. R.**, **Rosen, D. B.**, **Brdičková, N.**, **Xu, Y.**, **An, J.**, **Lanier, L. L.**, **Cyster, J. G. et al.**, CD69 acts downstream of interferon-α/β to inhibit S1P 1 and lymphocyte egress from lymphoid organs. *Nature* 2006. **440**: 540–544.

11 **Kamphuis, E.**, **Junt, T.**, **Waibler, Z.**, **Forster, R. and Kalinke, U.**, Type I interferons directly regulate lymphocyte recirculation and cause transient blood lymphopenia. *Blood* 2006. **108**: 3253–3261.

12 **Zhu, M. and Fu, Y X.**, The role of core TNF/LIGHT family members in lymph node homeostasis and remodeling. *Immunol. Rev.* 2011. **244**: 75–84.

13 **Tay, M. H. D.**, **Lim, S. Y. J.**, **Leong, Y. F. I.**, **Thiam, C. H.**, **Tan, K. W.**, **Torta, F. T.**, **Narayanaswamy, P. et al.**, Halted lymphocyte egress via efferent lymph contributes to lymph node hypertrophy during hypercholesterolemia. *Front. Immunol.* 2019. **10**: 1–14.

14 **Xie, J. H.**, **Nomura, N.**, **Koprak, S. L.**, **Quackenbush, E. J.**, **Forrest, M. J. and Rosen, H.**, Sphingosine-1-phosphate receptor agonism impairs the efficiency of the local immune response by altering trafficking of naive and antigen-activated CD4 + T cells. *J. Immunol.* 2003. **170**: 3662–3670.

15 **Mann, E. A.**, **Markovic, S. N. and Murasko, D M.**, Inhibition of lymphocyte recirculation by murine interferon: effects of various interferon preparations and timing of administration. *J. Interferon Res.* 1989. **9**: 35–51.

16 **Gresser, I.**, **Guy-Grand, D.**, **Maury, C. and Maunoury, M T.**, Interferon induces peripheral lymphadenopathy in mice. *J. Immunol.* 1981. **127**: 1569–1575.

17 **Young, A. J.**, **Seabrook, T. J.**, **Marston, W. L.**, **Dudler, L. and Hay, J B.**, A role for lymphatic endothelium in the sequestration of recirculating γδ T cells in TNF-α-stimulated lymph nodes. *Eur. J. Immunol.* 2000. **30**: 327–334.

18 **Zhu, M.**, **Yang, Y.**, **Wang, Y.**, **Wang, Z. and Fu, Y - X.**, LIGHT regulates inflamed draining lymph node hypertrophy. *J. Immunol.* 2011. **186**: 7156–7163.

19 **Wee, J. L. K.**, **Greenwood, D. L. V.**, **Han, X. and Scheerlinck, J P Y.**, Inflammatory cytokines IL-6 and TNF-α regulate lymphocyte trafficking through the local lymph node. *Vet. Immunol. Immunopathol.* 2011. **144**: 95–103.

20 **Cyster, J G.**, Chemokines, sphingosine-1-phosphate, and cell migration in secondary lymphoid organs. *Annu. Rev. Immunol.* 2005. **23**: 127–159.

21 **Nakai, A.**, **Hayano, Y.**, **Furuta, F.**, **Noda, M. and Suzuki, K.**, Control of lymphocyte egress from lymph nodes through β2-adrenergic receptors. *J. Exp. Med.* 2014. **211**: 2583–2598.

22 **Schulz, O.**, **Ugur, M.**, **Friedrichsen, M.**, **Radulovic, K.**, **Niess, J. H.**, **Jalkanen, S.**, **Krueger, A. et al.**, Hypertrophy of infected Peyer's patches arises from global, interferon-receptor, and CD69-independent shutdown of lymphocyte egress. *Mucosal Immunol*. 2014. **7**: 892–904.

23 **Deal, E. M.**, **Lahl, K.**, **Narváez, C. F. C.**, **Butcher, E. C.**, **Greenberg, H. B. and Narvaez, C F.**, Plasmacytoid dendritic cells promote rotavirus-induced human and murine B cell responses. *J. Clin. Invest*. 2013. **123**: 2464–2474.

24 **Trevejo, J. M.**, **Marino, M. W.**, **Philpott, N.**, **Josien, R.**, **Richards, E. C.**, **Elkon, K. B. and Falck-Pedersen, E.**, TNF-α-dependent maturation of local dendritic cells is critical for activating the adaptive immune response to virus infection. *Proc. Natl. Acad. Sci. USA* 2001. **98**: 12162–12167.

25 **Levy, D. E. and García-Sastre, A.**, The virus battles: IFN induction of the antiviral state and mechanisms of viral evasion. *Cytokine Growth Factor Rev*. 2001. **12**: 143–156.

26 **Mahlakõiv, T.**, **Hernandez, P.**, **Gronke, K.**, **Diefenbach, A. and Staeheli, P.**, Leukocyte-derived IFN-α/β and epithelial IFN-λ constitute a compartmentalized mucosal defense system that restricts enteric virus infections. *PLoS Pathog*. 2015. **11**: e1004782.

27 **Nakawesi, J.**, **This, S.**, **Hütter, J.**, **Boucard-Jourdin, M.**, **Barateau, V.**, **Muleta, K. G.**, **Gooday, L. J. et al.**, αvβ8 integrin-expression by

BATF3-dependent dendritic cells facilitates early IgA responses to Rotavirus. *Mucosal Immunol*. 2020. https://doi.org/10.1038/s41385-020-0276-8.

28 **Sun, T., Rojas, O. L., Li, C., Ward, L. A., Philpott, D. J. and Gommerman, J L.**, Intestinal Batf3-dependent dendritic cells are required for optimal antiviral T-cell responses in adult and neonatal mice. *Mucosal Immunol*. 2016. **10**: 1–14.

29 **Blutt, S. E., Warfield, K. L., Lewis, D. E., Conner, M E.**, Early response to rotavirus infection involves massive B cell activation. *J. Immunol.* 2002. **168**: 5716–5721.

30 **VanCott, J. L., Mcneal, M. M., Flint, J., Bailey, S. A., Choi, A. H. C. and Ward, R L.**, Role of T cell-independent B cell activity in the resolution of primary rotavirus infection in mice. *Eur. J. Immunol.* 2001. **31**: 3380–3387.

31 **Franco, M. A. and Greenberg, H B.**, Immunity to rotavirus infection in mice. *J Infect Dis*. 1999. **179**(Suppl): S466–9.

32 **Tomura, M., Yoshida, N., Tanaka, J., Karasawa, S., Miwa, Y., Miyawaki, A. and Kanagawa, O.**, Monitoring cellular movement in vivo with photoconvertible fluorescence protein 'Kaede' transgenic mice. *Proc. Natl. Acad. Sci. USA* 2008. **105**: 10871–10876.

33 **Cinamon, G., Matloubian, M., Lesneski, M. J., Xu, Y., Low, C., Lu, T., Proia, R. L. et al.**, Sphingosine 1-phosphate receptor 1 promotes B cell localization in the splenic marginal zone. *Nat. Immunol.* 2004. **5**: 713–720.

34 **Phan, T. G., Amesbury, M., Gardam, S., Crosbie, J., Hasbold, J., Hodgkin, P. D., Basten, A. et al.**, B cell receptor-independent stimuli trigger immunoglobulin (Ig) class switch recombination and production of IgG autoantibodies by anergic self-reactive B cells. *J. Exp. Med.* 2003. **197**: 845–860.

35 **Park, C., Hwang, I. Y., Sinha, R. K., Kamenyeva, O., Davis, M. D. and Kehrl, J H.**, Lymph node B lymphocyte trafficking is constrained by anatomy and highly dependent upon chemoattractant desensitization. *Blood*. 2012. **119**: 978–989.

36 **Harp, J. R., Gilchrist, M. A. and Onami, T M.**, Memory T cells are enriched in lymph nodes of selectin-ligand–deficient mice. *J. Immunol.* 2010. **185**: 5751–5761.

37 **Cyster, J. G. and Schwab, S R.**, Sphingosine-1-phosphate and lymphocyte egress from lymphoid organs. *Annu. Rev. Immunol.* 2012. **30**: 69–94.

38 **McLachlan, J. B., Hart, J. P., Pizzo, S V., Shelburne, C. P., Staats, H. F., Gunn, M. D. and Abraham, S N.**, Mast cell-derived tumor necrosis factor induces hypertrophy of draining lymph nodes during infection. *Nat. Immunol.* 2003. **4**: 1199–1205.

39 **Kunder, C. A., St. John, A. L., Li, G., Leong, K. W., Berwin, B., Staats, H. F. and Abraham, S. N.**. Mast cell-derived particles deliver peripheral signals to remote lymph nodes. *J. Exp. Med.* 2009. **206**: 2455–2467.

40 **Girard, J. P., Moussion, C. and Förster, R.**, HEVs, lymphatics and homeostatic immune cell trafficking in lymph nodes. *Nat. Rev. Immunol.* 2012. **12**: 762–773.

41 **Li, C., Lam, E., Perez-Shibayama, C., Ward, L. A., Zhang, J., Lee, D., Nguyen, A. et al.**, Early-life programming of mesenteric lymph node stromal cell identity by the lymphotoxin pathway regulates adult mucosal immunity. *Sci. Immunol.* 2019. **4**: 1–18.

42 **Mackay, C. R., Marston, W. and Dudler, L.**, Altered patterns of T cell migration through lymph nodes and skin following antigen challenge. *Eur. J. Immunol.* 1992. **22**: 2205–2210.

43 **Lauzurica, P., Sancho, D., Torres, M., Albella, B., Marazuela, M., Merino, T., Bueren, J. A. et al.**, Phenotypic and functional characteristics of hematopoietic cell lineages in CD69-deficient mice. *Blood*. 2000. **95**: 2312–2320.

44 **Martín-Fontecha, A., Sebastiani, S., Höpken, U. E., Uguccioni, M., Lipp, M., Lanzavecchia, A. and Sallusto, F.**, Regulation of dendritic cell migration to the draining lymph node: Impact on T lymphocyte traffic and priming. *J. Exp. Med.* 2003. **198**: 615–621.

45 **Hägerbrand, K., Westlund, J., Yrlid, U., Agace, W. and Johansson-Lindbom, B.**. MyD88 signaling regulates steady-state migration of intestinal CD103+ dendritic cells independently of TNF-α and the gut microbiota. *J. Immunol.* 2015. **195**: 2888–2899.

46 **López, A. G., Bekiaris, V., Luda, K. M., Hütter, J., Ulmert, I., Muleta, K. G., Nakawesi, J. et al.**, Migration of murine intestinal dendritic cell subsets upon intrinsic and extrinsic TLR3 stimulation. *Eur. J. Immunol.* 2020. https://onlinelibrary.wiley.com/doi/abs/10.1002/eji.201948497. https://doi.org/10.1002/eji.201948497.

47 **Dudeck, J., Ghouse, S. M., Lehmann, C. H. K., Hoppe, A., Schubert, N., Nedospasov, S. A., Dudziak, D. et al.**, Mast-cell-derived TNF amplifies CD8+ dendritic cell functionality and CD8+ T cell priming. *Cell Rep*. 2015. **13**: 399–411.

48 **Suto, H., Nakae, S., Kakurai, M., Sedgwick, J. D., Tsai, M. and Galli, S J.**, Mast cell-associated TNF promotes dendritic cell migration. *J. Immunol.* 2014. **176**: 4102–4112.

49 **Demeure, C. E., Brahimi, K., Hacini, F., Marchand, F., Péronet, R., Huerre, M., St.-Mezard, P. et al.**, Anopheles mosquito bites activate cutaneous mast cells leading to a local inflammatory response and lymph node hyperplasia . *J. Immunol.* 2005. **174**: 3932–3940.

50 **Dawicki, W., Jawdat, D. W., Xu, N. and Marshall, J S.**, Mast cells, histamine, and IL-6 regulate the selective influx of dendritic cell subsets into an inflamed lymph node. *J. Immunol.* 2010. **184**: 2116–2123.

51 **Matloubian, M., Lo, C. G., Cinamon, G., Lesneski, M. J., Xu, Y., Brinkmann, V., Allende, M. L. et al.**, Lymphocyte egress from thymus and peripheral lymphoid organs is dependent on S1P receptor 1. *Nature*. 2004. **427**: 355–360.

52 **Wieduwild, E., Girard-Madoux, M. J., Quatrini, L., Laprie, C., Chasson, L., Rossignol, R., Bernat, C. et al.**, B2-adrenergic signals downregulate the innate immune response and reduce host resistance to viral infection. *J. Exp. Med.* 2020. **217**. https://doi.org/10.1084/jem.20190554.

53 **Gabanyi, I., Muller, P. A., Feighery, L., Oliveira, T. Y., Costa-Pinto, F. A. and Mucida, D.**, Neuro-immune interactions drive tissue programming in intestinal macrophages. *Cell*. 2016. **164**: 378–391.

54 **Binns, R. M. and Licence, S T.**, Exit of recirculating lymphocytes from lymph nodes is directed by specific exit signals. *Eur. J. Immunol.* 1990. **20**: 449–452.

55 **Peschon, J. J., Torrance, D. S., Stocking, K. L., Glaccum, M. B., Otten, C., Willis, C. R., Charrier, K. et al.**, TNF receptor-deficient mice reveal divergent roles for p55 and p75 in several models of inflammation. *J. Immunol.* 1998. **160**: 943–952.

Abbreviations: **β2AR**: β2-adrenergic receptor · **HEL**: hen egg lysozyme · **mLN**: mesenteric LN · **pLN**: peripheral LN · **PP**: Peyer's patche · **RV**: rotavirus · **S1P**: sphingosine-1 phosphate · **TNFR**: TNF receptor

Full correspondence: Dr. Katharina Lahl, Immunology Section, Lund University, Möllevångsvägen 6F, 222 40 Lund, Sweden
e-mail: klah@dtu.dk

Received: 22/9/2020
Revised: 24/11/2020
Accepted: 21/12/2020
Accepted article online: 22/12/2020